SLAC-PUB-12809
September 2007

External inverse-Compton emission from blazar jets

Jennifer E. Carson and James Chiang

Submitted to Astrophysical Journal

Stanford Linear Accelerator Center, Stanford University, Stanford, CA 94309

Work supported by Department of Energy contract DE–AC02–76SF00515.

ABSTRACT

According to leptonic models for the high-energy emission from blazars, relativistic electrons in the inner jets inverse-Compton scatter photons from a variety of sources. Seed photons are certainly introduced via the synchrotron process from the electrons themselves, but external sources of seed photons may also be present. In this paper, we present detailed derivations of the equations describing external inverse-Compton scattering from two sources of seed photons: direct emission from the accretion disk, and accretion disk photons that have scattered off the broad line region. For each source, we derive the seed photon spectrum incident on the jet, the single electron energy loss rate, and the emitted photon spectrum.

Subject headings: BL Lacertae Objects: general — galaxies: jets — radiation mechanisms: non-thermal

1. Introduction

The Energetic Gamma-Ray Explorer Telescope (EGRET) aboard the Compton Gamma-Ray Observatory detected dozens of blazars above 100 MeV (Hartman *et al.* 1999), most of which are flat-spectrum radio quasars (FSRQs). It was found that in order to fit the observed broadband spectral energy distributions (SEDs) of many FSRQs using leptonic models, especially during flares, it was necessary to introduce a substantial contribution from external inverse-Compton (EIC) emission to the high-energy SED. In the EIC scenario, the photons available for inverse-Compton scattering in the inner jet are seeded not only from the synchrotron-emitting electrons themselves (synchrotron self-Compton, or SSC), but also from external sources such as the accretion disk (*cf.* Hartman *et al.* (2001)). Such a scenario is expected in FSRQs, where the disk emission is often very strong.

The imminent launch of the Gamma-Ray Large Area Space Telescope (GLAST), with its main instrument, the Large Area Telescope (LAT, 30 MeV - 300 GeV), will open the gamma-ray sky to the detection of hundreds to thousands of new sources, the majority of which will probably be blazars. Sophisticated model fitting will be required to extract the underlying physics from the wealth of new spectral data. Motivated by the potential of the LAT, we are developing a code that models the leptonic radiation processes from the inner jets of blazars; this code is an expansion of the work of M. Böttcher (Böttcher, Mause, and Schlickeiser 1997; Böttcher and Bloom 2000; Hartman *et al.* 2001). As part of the code development, this paper derives the equations for the electron energy losses and emitted spectra expected from external inverse-Compton emission from two external sources of soft seed photons. First, we consider accretion disk photons incident directly on the jet. We then consider photons that scatter off the broad line region (BLR) and into the jet beam. Many of these derivations are not new and have been used in the past. However, complete derivations of these two EIC processes have not been available in the literature, and we

hope that collecting the various equations here will support and document the code that implements them.

Both the derivations in this paper and the code itself employ only very minimal approximations. In particular, the geometric treatment of the emission due to BLR-scattered photons is much more general than what has been available to date. We also note that the derivation of the direct disk EIC emission corrects some minor errors found in the literature. Where the derivations restate previous results, we cite the original source.

The paper contains two main sections, one devoted to the direct disk EIC emission (§2), and one devoted to the BLR-scattered EIC emission (§3). Within each section, we derive expressions for the photon spectrum incident on the jet, the single electron energy loss rate, and the emitted inverse-Compton spectrum.

2. External inverse-Compton scattering of accretion disk photons

In this section we derive the equations describing inverse-Compton scattering of accretion disk photons incident directly on the jet ("external Compton from the disk", or ECD). In §2.1, we lay out an expression for the accretion disk spectrum encountered by the jet blob. We then derive the full expression for the energy loss rate for a single electron (§2.2), the loss rate in the Thomson limit (§2.3), and the loss rate simplified by a few minor approximations (§2.4). Many of the derivations in these four sections are expansions (with corrections) of the equations in Böttcher, Mause, and Schlickeiser (1997) (hereafter BMS97); in §2.5, we summarize the differences between our final expressions and the ones in that paper. Finally, we derive both expression for the emitted ECD spectrum (§2.6). We adopt the notation of BMS97 throughout this paper.

Figure 1 shows the basic geometry of the jet and accretion disk. We define two frames:

the frame in which the relativistically-moving blob is at rest (unprimed) and the rest frame of the relativistic electron in the blob (primed). There are several angles associated with each frame, as depicted in Figure 2. The quantity ϕ, defined in the blob frame, is the azimuthal angle about the direction of motion of the blob between the photon direction and the electron direction of motion. The quantity ϕ'_s, defined in the electron rest frame, is the azimuthal angle about the incoming photon direction between the scattered photon direction and the direction of motion of the blob frame with respect to the stationary electron. It is also useful to define several cosines:

$$\eta_e = \cos\theta_e \tag{1a}$$

$$\eta_{ph} = \cos\theta_{ph} \tag{1b}$$

$$\mu = \cos\psi = \eta_{ph}\eta_e + \sin\theta_{ph}\sin\theta_e\cos\phi \tag{1c}$$

$$\kappa' = \cos\chi' \tag{1d}$$

$$\mu' = \cos\psi' \tag{1e}$$

$$\mu'_s = \cos\psi'_s = \kappa'\mu' + \sin\chi'\sin\psi'\cos\phi'_s \tag{1f}$$

(*cf.* equations 6 and 7 of BMS97).

2.1. Seed photon flux from the accretion disk

The emission from the surface of an optically thick, geometrically thin accretion disk is derived in Shakura and Sunyaev (1973); from equation 2.6 of that work, the energy flux from the disk surface is

$$Q = \frac{3}{8\pi}\dot{M}\frac{GM}{R^3}\left(1-\sqrt{\frac{R_0}{R}}\right) \ , \tag{2}$$

where $R_0 \equiv 6R_g = \frac{6GM}{c^2}$, M is the black hole mass, $\dot{M}$ is the accretion rate, and R is the disk radius. We determine the temperature profile by assuming that each annulus of the

disk radiates as a blackbody,

$$Q = \sigma T^4(R) \ , \tag{3}$$

where σ is the Stefan-Boltzmann constant. Casting Q in a more convenient format,

$$Q = Q \times \left(\frac{R_g}{GM/c^2}\right)^3 = \frac{3c^2}{8\pi G^2}\frac{\dot{M}}{M^2}\left(\frac{R_g}{R}\right)^3\left(1-\sqrt{\frac{R_0}{R}}\right) \ , \tag{4}$$

and solving equation 3 for $T(R)$, we find

$$\Theta(R) \equiv \frac{\mathrm{k}_b T(R)}{m_e c^2} = 1.44\left(\frac{M}{M_\odot}\right)^{-\frac{1}{2}}\left(\frac{\dot{M}}{M_\odot/yr}\right)^{\frac{1}{4}}\left(\frac{R}{R_g}\right)^{-\frac{3}{4}}\left(1-\sqrt{\frac{6R_g}{R}}\right)^{\frac{1}{4}} \tag{5}$$

(*cf.* equation 4 of BMS97).

To derive the differential accretion disk flux, we begin with the standard blackbody expression for the differential energy density (Rybicki and Lightman (1979), equations 1.50 and 1.51),

$$B_\nu = \frac{d^2u}{d\nu d\Omega} = \frac{2h\nu^3/c^3}{e^{h\nu/kT}-1} \ , \tag{6}$$

where $T = T(R)$ in our case, and convert to a number density by dividing by the energy $h\nu$. Then, the differential accretion disk flux is

$$\frac{d^2n_{ph}}{d\nu d\Omega} = \frac{2\nu^2/c^3}{e^{h\nu/kT}-1} = \frac{2}{c^3}\left(\frac{m_e c^2}{h}\right)\frac{\epsilon^{*2}}{e^{\epsilon^*/\theta(R)}-1} \ , \tag{7}$$

expressed in terms of a dimensionless photon energy $\epsilon^* \equiv \frac{h\nu^*}{m_e c^2}$. Here we have introduced yet another frame of reference, the frame of the accretion disk (*i.e.* the lab frame), denoted with an asterisk.

Next we convert to a differential in energy $d\epsilon^*$, where $d\nu^* = \frac{m_e c^2}{h}d\epsilon^*$, to obtain

$$\left(\frac{d^2n_{ph}}{d\epsilon d\Omega}\right)^* = \frac{2}{c^3}\left(\frac{m_e c^2}{h}\right)^3\frac{\epsilon^{*2}}{e^{\epsilon^*/\Theta(R)}-1} \ . \tag{8}$$

To evaluate the electron losses from this accretion disk flux (see §2.2), equation 8 should be transformed to the blob frame. The Lorentz invariant quantity in the transformation is

$\frac{I_\nu}{\nu^3}$ where I_ν is the energy density (Rybicki and Lightman (1979), equation 4.110), so

$$\frac{d^2n_{ph}}{d\epsilon d\Omega} = \frac{\epsilon^2}{\epsilon^{*2}}\left(\frac{d^2n_{ph}}{d\epsilon d\Omega}\right)^* = \frac{2}{c^3}\left(\frac{m_e c^2}{h}\right)^3 \frac{\epsilon^2}{e^{\frac{\epsilon\Gamma(1+\beta_\Gamma\eta_{ph})}{\Theta(R)}} - 1} \ , \tag{9}$$

where $\Gamma = \frac{1}{\sqrt{1-\beta_\Gamma^2}}$ is the bulk Lorentz factor of the blob and we have used the Doppler formula (equation A1) to convert ϵ^* to ϵ.

2.2. Single electron energy loss

With the angles defined according to Figure 2, we can set up the energy loss equation for a single electron with Lorentz factor $\gamma = \frac{1}{\sqrt{1-\beta^2}}$ (in the blob frame):

$$\begin{aligned} -\left(\frac{d\gamma}{dt}\right)_{IC} &= \frac{c}{2}\int_{-1}^{1} d\eta_e \int_{4\pi} d\Omega_{ph} \int_0^\infty d\epsilon \int_{-1}^{1} d\kappa' \int_0^\infty d\epsilon'_s \int_0^{2\pi} d\phi'_s \\ &\times \ (1-\beta\mu)\frac{d^2n_{ph}}{d\epsilon d\Omega_{ph}} \frac{d^2\sigma_{KN}}{d\Omega'_{ph,s} d\epsilon'_s}\left[\gamma\epsilon'_s(1+\beta\mu'_s) - \epsilon\right] \\ &= \frac{c}{2}\int_{-1}^{1} d\eta_e \int_{4\pi} d\Omega_{ph} \int_0^\infty d\epsilon \int_{-1}^{1} d\kappa'(1-\beta\mu)\frac{d^2n_{ph}}{d\epsilon d\Omega_{ph}} \times I_2 \ , \end{aligned} \tag{10}$$

(*cf.* equation 5 of BMS97), where $d\Omega_{ph} \equiv \int d\eta_{ph} \int d\phi$[1], $\frac{d^2n_{ph}}{d\epsilon d\Omega_{ph}}$ is the differential number of accretion disk photons and $\frac{d\sigma_{KN}}{d\Omega'_{ph,s}}$ is the full Klein-Nishina cross section for photon scattering off of free electrons. I_2 is given by equation 15.

Equation 10 first integrates in the electron rest frame over all scattering angles (κ' and ϕ'_s) and scattered photon energies (ϵ'_s), and then, in the blob frame, it integrates over all incident photon energies (ϵ) and directions (η_{ph} and ϕ). The factor $[\gamma\epsilon'_s(1+\beta\mu'_s) - \epsilon]$ in equation 10 is the energy loss due to one scattering event, $\epsilon_s - \epsilon$, where ϵ_s is expressed in terms of ϵ'_s via the Doppler formula (equation A1). The integral $\frac{1}{2}\int_{-1}^{1} d\eta_e$ computes the average electron energy loss from the ensemble of electrons with an isotropic angular

[1]We adopt the notation $\Omega_{ph} = (\eta_{ph}, \phi)$ throughout this paper.

distribution. The factor $c(1-\beta\mu)$ is the relative velocity between the electron and the photon along the electron direction of motion. It is necessary since we are computing the rate in the frame in which the electron is moving (*cf.* equation 2.11 of Blumenthal & Gould (1970)).

We will first integrate over the scattered photon quantities in the electron rest frame (ϕ'_s and ϵ'_s). We can immediately integrate over ϕ'_s, the azimuthal angle in the electron rest frame, as its dependence is only in the last factor. Substituting for μ'_s in that factor (via equation 1f), we have

$$\begin{aligned} I_1 &\equiv \int_0^{2\pi} d\phi'_s \left[\gamma\epsilon'_s(1+\beta\mu'_s) - \epsilon\right] \\ &= \int_0^{2\pi} d\phi'_s \left[\gamma\epsilon'_s(1+\beta\kappa'\mu') - \epsilon + \gamma\epsilon'_s\beta\sin\chi'\sin\psi'\cos\phi'_s\right] \\ &= 2\pi[\gamma\epsilon'_s(1+\beta\kappa'\mu') - \epsilon] \ . \end{aligned} \tag{11}$$

Next we will do the integration over ϵ'_s, which depends on equation 11 above and the scattering cross section. The differential Klein-Nishina cross section for light that is initially unpolarized scattering off an electron at rest is

$$\frac{d^2\sigma_{KN}}{d\Omega'_{ph,s}d\epsilon'_s} = \frac{r_e^2}{2}\frac{\epsilon_s'^2}{\epsilon'^2}\left(\frac{\epsilon'}{\epsilon'_s} + \frac{\epsilon'_s}{\epsilon'} - \sin^2\chi'\right)\delta\left(\epsilon'_s - \frac{\epsilon'}{1+\epsilon'(1-\kappa')}\right) \tag{12}$$

(*cf.* Heitler (1984), eq. 39 (p. 219) and eq. 4 (p. 211)), where the delta function relates the incident and inverse-Compton-scattered photon energies for a electron at rest:

$$\epsilon'_s = \frac{\epsilon'}{1+\epsilon'(1-\kappa')} \ . \tag{13}$$

Plugging equation 13 into equation 12 to express the cross section entirely in terms of the scattered photon energy ϵ'_s, we have

$$\frac{d\sigma_{KN}}{d\Omega'_{ph,s}} = \frac{r_e^2}{2}[f^3 - (1-\kappa'^2)f^2 + f] \ , \tag{14}$$

where $f \equiv 1 - \epsilon'_s(1-\kappa')$. Collecting the terms that depend on ϵ'_s, we have

$$\begin{aligned} I_2 &\equiv \int_0^\infty \frac{d\sigma_{KN}}{d\Omega'_{ph,s}}\,\delta\left(\epsilon'_s - \frac{\epsilon'}{1+\epsilon'(1-\kappa')}\right) d\epsilon'_s \times I_1 \\ &= \pi r_e^2 \int d\epsilon'_s\,\delta\left(\epsilon'_s - \frac{\epsilon'}{1+\epsilon'(1-\kappa')}\right) \\ &\times \left[f^3 - (1-\kappa'^2)f^2 + f\right] \times \left[\gamma\epsilon'_s(1+\beta\kappa'\mu') - \epsilon\right] , \end{aligned} \tag{15}$$

where I_1 is given by equation 11.

Before evaluating equation 15, we make two changes of variables. In equation 10 we will integrate over incident photon energies and directions in the *blob* frame. However, equation 15 expresses incident energies ϵ' and directions μ' in the *electron* rest frame. We convert ϵ' to ϵ with the Doppler formula (equation A1),

$$\epsilon' = \frac{\epsilon(1-\beta\mu)}{\sqrt{1-\beta^2}} = \epsilon\gamma(1-\beta\mu) , \tag{16}$$

so

$$\frac{\epsilon'}{1+\epsilon'(1-\kappa')} = \frac{\epsilon\gamma(1-\beta\mu)}{1+\epsilon\gamma(1-\beta\mu)(1-\kappa')} = \frac{\epsilon\gamma(1-\beta\mu)}{F} , \tag{17}$$

where $F \equiv 1 + \epsilon\gamma(1-\beta\mu)(1-\kappa')$. The delta function in equation 15 becomes

$$\delta\left(\epsilon'_s - \frac{\epsilon'}{1+\epsilon'(1-\kappa')}\right) = \delta\left(\epsilon'_s - \frac{\epsilon\gamma(1-\beta\mu)}{F}\right) . \tag{18}$$

We convert μ' to μ using the abberation formula (equation A2), so

$$\gamma(1+\beta\kappa'\mu') = \gamma\left(1 + \frac{\beta\kappa'(\mu-\beta)}{1-\beta\mu}\right) . \tag{19}$$

Finally, evaluating the components of equation 15, we have

$$\begin{aligned} f &= 1 - \epsilon'_s(1-\kappa') = 1 - \frac{\epsilon\gamma(1-\beta\mu)(1-\kappa')}{F} = \frac{1}{F} , \\ \gamma\epsilon'_s(1+\beta\kappa'\mu') &= \gamma\left(\frac{\epsilon\gamma(1-\beta\mu)}{F}\right)\left(1 + \frac{\beta\kappa'(\mu-\beta)}{1-\beta\mu}\right) = \frac{\epsilon\gamma^2(1-\beta\mu+\beta\kappa'(\mu-\beta))}{F} , \end{aligned}$$

and

$$I_2 = \pi r_e^2 \left(\frac{1}{F^3} - \frac{1-\kappa'^2}{F^2} + \frac{1}{F}\right) \times \epsilon \left(\frac{\gamma^2[1-\beta\mu+\beta\kappa'(\mu-\beta)]}{F} - 1\right)$$
$$= \pi r_e^2 \epsilon \left(\frac{1+F(F-1)+F\kappa'^2}{F^3}\right) \times \left(\frac{\gamma^2[1-\beta\mu+\beta\kappa'(\mu-\beta)]}{F} - 1\right) . \quad (20)$$

Plugging I_2 back into equation 10, we have

$$-\left(\frac{d\gamma}{dt}\right)_{ECD} = \frac{c}{2}\pi r_e^2 \int_{-1}^{1} d\eta_e \int_{\eta_{ph,min}}^{\eta_{ph,max}} d\eta_{ph} \int_0^{2\pi} d\phi \int_0^{\infty} d\epsilon \int_{-1}^{1} d\kappa'(1-\beta\mu) \times$$
$$\frac{d^2 n_{ph}}{d\epsilon d\Omega_{ph}} \epsilon \left(\frac{1+F(F-1)+F\kappa'^2}{F^3}\right) \times \left(\frac{\gamma^2[1-\beta\mu+\beta\kappa'(\mu-\beta)]}{F} - 1\right) , \quad (21)$$

where $\eta_{ph,min}$ and $\eta_{ph,max}$ are determined by the inner and outer disk radius, respectively. Note that except for the limits on η_{ph}, this expression is still generally valid, since we have not specified $\frac{d^2 n_{ph}}{d\epsilon d\Omega_{ph}}$.

The integration over the accretion disk photons should be performed in terms of ϵ, the incident photon energies in the blob frame, and R, the disk radius. To obtain an expression for the disk photon integrals that depends only on these two quantities, we first express η_{ph}, the direction cosine of the incident photons with respect to the jet axis (or blob direction) in the blob frame, in terms of R, and then we convert $d\eta_{ph}$ in the blob frame to dR in the accretion disk frame.

The direction cosine for the incident photons in the accretion disk frame is $\eta^*_{ph} = \frac{z}{\sqrt{R^2+z^2}}$, where z is the height of the scattering site above the disk (see Figure 1). This is converted to the blob frame via the abberation formula (equation A2),

$$\eta_{ph} = \frac{\eta^*_{ph} - \beta_\Gamma}{1 - \beta_\Gamma \eta^*_{ph}} = \frac{z - \beta_\Gamma\sqrt{R^2+z^2}}{\sqrt{R^2+z^2} - \beta_\Gamma z} = \frac{z - \beta_\Gamma x}{x - \beta_\Gamma z} , \quad (22)$$

where $x \equiv \sqrt{R^2+z^2}$ (*cf.* BMS97, equation 11). For $d\eta_{ph}$ we derive

$$d\eta_{ph} = \frac{\partial \eta_{ph}}{\partial R} dR = \frac{-1}{\Gamma^2} \times \frac{zR\,dR}{x(x-\beta_\Gamma z)^2} . \quad (23)$$

Using equations 9, 22, and 23, we find for equation 21:

$$-\left(\frac{d\gamma}{dt}\right)_{ECD} = \frac{\pi r_e^2}{\Gamma^2 c^2}\left(\frac{m_e c^2}{h}\right)^3 \int_{-1}^{1} d\eta_e \int_{R_{min}}^{R_{max}} \frac{zR\,dR}{x(x-\beta_\Gamma z)^2} \int_0^{2\pi} d\phi \int_0^{\infty} d\epsilon \, \frac{\epsilon^3}{e^{\frac{\epsilon\Gamma(1+\beta_\Gamma\eta_{ph})}{\Theta(R)}}-1} \times \int_{-1}^{1} d\kappa' \;\; (1-\beta\mu)\left(\frac{1+F(F-1)+F\kappa'^2}{F^3}\right)\left(\frac{\gamma^2[1-\beta\mu+\beta\kappa'(\mu-\beta)]}{F}-1\right) \;, \quad (24)$$

where $x \equiv \sqrt{R^2+z^2}$, $F \equiv 1+\epsilon\gamma(1-\beta\mu)(1-\kappa')$, and R_{min} and R_{max} are the inner and outer edges of the disk, respectively. This is the final, exact expression for the energy loss rate of one electron due to inverse-Compton scattering of accretion disk photons incident directly on the jet blob.

2.3. Thomson limit for the electron loss rate

In the Thomson limit, $\epsilon\gamma \ll 1$ and $F \approx 1$. In this limit, and neglecting terms of order $\frac{1}{\gamma^2}$, the last two factors of equation 24 are greatly simplified:

$$\left(\frac{1+F(F-1)+F\kappa'^2}{F^3}\right)\left(\frac{\gamma^2[1-\beta\mu+\beta\kappa'(\mu-\beta)]}{F}-1\right) \approx (1+\kappa'^2)\gamma^2[1-\beta\mu+\beta\kappa'(\mu-\beta)]$$
$$\approx \gamma^2(1+\kappa'^2)(1-\beta\mu)(1-\kappa') \;.$$

With this approximation, we have

$$-\left(\frac{d\gamma}{dt}\right)_{ECD,Thomson} = \frac{\pi r_e^2\gamma^2}{\Gamma^2 c^2}\left(\frac{m_e c^2}{h}\right)^3 \int_{-1}^{1} d\eta_e \int_{R_{min}}^{R_{max}} \frac{zR\,dR}{x(x-\beta_\Gamma z)^2} \int_0^{2\pi} d\phi \int_0^{\infty} d\epsilon \, \frac{\epsilon^3}{e^{\frac{\epsilon\Gamma(1+\beta_\Gamma\eta_{ph})}{\Theta(R)}}-1} \times \int d\kappa'(1-\beta\mu)^2(1+\kappa'^2)(1-\kappa') \;. \quad (25)$$

The integrals over ϵ, κ', ϕ, and η_e are straightforward to evaluate:

$$\int_0^{\infty} d\epsilon \, \frac{\epsilon^3}{e^{\frac{\epsilon\Gamma(1+\beta_\Gamma\eta_{ph})}{\Theta(R)}}-1} = \frac{\Gamma(4)\zeta(4)}{\Gamma^4}\left(\frac{\Theta(R)}{1+\beta_\Gamma\eta_{ph}}\right)^4 = \frac{\pi^4}{15\Gamma^4}\left(\frac{\Theta(R)}{1+\beta_\Gamma\eta_{ph}}\right)^4 \;, \quad (26)$$

where $\Gamma(4) = 6$ and ζ is the Reimann Zeta function. Substituting the expression for η_{ph} from equation 22, we find

$$\frac{1}{1+\beta_\Gamma\eta_{ph}} = \Gamma^2\frac{x-\beta_\Gamma z}{x} \quad (27)$$

and

$$\int_0^\infty d\epsilon \, \frac{\epsilon^3}{e^{\frac{\epsilon\Gamma(1+\beta_\Gamma\eta_{ph})}{\Theta(R)}} - 1} = \frac{\pi^4\Gamma^4\Theta^4(R)(x-\beta_\Gamma z)^4}{15x^4} \ . \tag{28}$$

Also,

$$\int_{-1}^{1} d\kappa'(1+\kappa'^2)(1-\kappa') = \frac{8}{3} \ , \tag{29}$$

and

$$\begin{aligned} \int_0^{2\pi} d\phi(1-\beta\mu)^2 &\approx \int_0^{2\pi} (1+\mu^2-2\beta\mu)d\phi \\ &= 2\pi(1+\eta_{ph}^2\eta_e^2-2\beta\eta_{ph}\eta_e) + \pi\sin^2\theta_{ph}\sin^2\theta_e \ , \end{aligned} \tag{30}$$

neglecting terms of order $\frac{1}{\gamma^2}$. Integrating equation 30 over η_e, we have

$$\pi\int_{-1}^{1} d\eta_e \left[2(1+\eta_{ph}^2\eta_e^2-2\beta\eta_{ph}\eta_e) + \sin^2\theta_{ph} - \sin^2\theta_{ph}\eta_e^2\right] = \frac{16\pi}{3} \ . \tag{31}$$

We are left with only the integral over R. Collecting equations 28, 29, and 31, equation 25 becomes

$$-\left(\frac{d\gamma}{dt}\right)_{ECD,Thomson} = \frac{16\pi^5\sigma_T\Gamma^2\gamma^2}{45c^2}\left(\frac{m_ec^2}{h}\right)^3 \int_{R_{min}}^{R_{max}} dR \frac{zR\Theta^4(R)(x-\beta_\Gamma z)^2}{x^5} \ , \tag{32}$$

where we have replaced r_e^2 with $\frac{3\sigma_T}{8\pi}$.

2.4. Analytic integration with minimal approximations

We can evaluate most of equation 24 analytically with three approximations. First, the function $\epsilon^3\left(e^{\frac{\epsilon\Gamma(1+\beta_\Gamma\eta_{ph})}{\Theta(R)}}-1\right)^{-1}$ is extremely narrowly peaked compared to the other functions in equation 24. We therefore approximate it as a delta function (*cf.* Böttcher and Bloom (2000), equation A6):

$$\frac{\epsilon^3}{e^{\frac{\epsilon\Gamma(1+\beta_\Gamma\eta_{ph})}{\Theta(R)}} - 1} \rightarrow A\delta(\epsilon - <\epsilon>) \ , \tag{33}$$

where

$$A = \int_0^\infty d\epsilon \, \frac{\epsilon^3}{e^{\frac{\epsilon\Gamma(1+\beta_\Gamma\eta_{ph})}{\Theta(R)}} - 1} = \frac{\pi^4\Gamma^4\Theta^4(R)(x-\beta_\Gamma z)^4}{15x^4} \tag{34}$$

(*cf.* equation 28), $<\epsilon>$ is the average photon energy at R,

$$<\epsilon>(R) = \frac{\int_0^\infty \epsilon\, n(\epsilon)d\epsilon}{\int_0^\infty n(\epsilon)d\epsilon} \ , \tag{35}$$

and $n(\epsilon)$ is the (blackbody) disk flux in the lab frame. Using equation 8 for $n(\epsilon)$, we have

$$<\epsilon>(R) = \frac{\Gamma(4)\zeta(4)}{\Gamma(3)\zeta(3)}\frac{\Theta(R)}{(1+\beta_\Gamma\eta_{ph})\Gamma} \simeq \frac{2.7}{\Gamma}\frac{\Theta(R)}{(1+\beta_\Gamma\eta_{ph})} \ . \tag{36}$$

The second approximation is to neglect terms of order $\frac{1}{\gamma^2}$. Then the last term in equation 24 becomes

$$\frac{\gamma^2(1-\beta\mu+\beta\kappa'(\mu-\beta))}{F} - 1 \approx \frac{\gamma^2(1-\beta\mu)(1-\kappa')}{F} \ . \tag{37}$$

The third approximation is to replace the integral that averages over η_e, $\frac{1}{2}\int_{-1}^{1} d\eta_e$, by setting $\eta_e = 0$. Then,

$$\mu = \eta_{ph}\eta_e + \sin\theta_{ph}\sin\theta_e\cos\phi \approx \cos\phi\sqrt{1-\eta_{ph}^2} \ . \tag{38}$$

With these three approximations, we have

$$\begin{aligned} -\left(\frac{d\gamma}{dt}\right)_{ECD,approx} &= \frac{\pi^4\sigma_T\Gamma^2\gamma^2}{20c^2}\left(\frac{m_e c^2}{h}\right)^3 \int_{R_{min}}^{R_{max}} dR \frac{zR\Theta^4(R)(x-\beta_\Gamma z)^2}{x^5} \\ &\times \ I(<\epsilon>,\gamma,\eta_{ph}) \ , \end{aligned} \tag{39}$$

where

$$\begin{aligned} I(<\epsilon>,\gamma,\eta_{ph}) &\equiv \int_0^{2\pi} d\phi(1-\beta\mu)^2 \int_{-1}^{1} d\kappa'(1-\kappa')\frac{1+F(F-1)+F\kappa'^2}{F^4} \ , \qquad (40) \\ \mu &= \sqrt{1-\eta_{ph}^2}\cos\phi \ , \\ F &= 1+\epsilon\gamma(1-a\cos\phi)(1-\kappa') \ , \\ a &\equiv \beta\sqrt{1-\eta_{ph}^2} \ , \qquad (41) \end{aligned}$$

and we have replaced r_e^2 with $\frac{3\sigma_T}{8\pi}$. The integrals in I can be solved analytically, as shown in BMS97, equations 15 and 16.

2.5. Comparison of electron loss expressions with BMS97

Before moving on to the derivation of the ECD spectrum emitted by the blob, we summarize the differences betewen the expressions for the single electron energy loss rate derived in this paper and those of BMS97.

1. Equation 9 for the accretion disk flux differs from equation 8 of BMS97 in two ways. First, they have a factor of 2 in the denominator, whereas we find that the factor of 2 should be in the numerator, making our expression larger by a factor of 4. Second, and more importantly, they include a factor of $\frac{1+\beta_\Gamma \eta_{ph}}{\eta_{ph}+\beta_\Gamma}$ which we do not find in our expression for the accretion disk flux.

2. Equation 24, the full expression for the electron loss rate, is larger than equation 9 of BMS97 by the factor of 4 that propogated through from the disk flux difference (see item 1 above). Also, we find that the BMS97 equation 9 must be multiplied by the factor $\frac{1+\beta_\Gamma \eta_{ph}}{\eta_{ph}+\beta_\Gamma}$ in order to agree with our expression. That is, if we were to use their equation 8 for the disk flux to derive their equation 9 for the loss rate, then the latter would differ from ours by two factors of $\frac{1+\beta_\Gamma \eta_{ph}}{\eta_{ph}+\beta_\Gamma}$.

3. BMS97 are internally consistent in deriving the Thomson approximation (their equation 12) from the full loss rate (their equation 9). Therefore, our equation 32 for the Thomson approximation differs from their equation 12 by the same factors of 4 and $\frac{1+\beta_\Gamma \eta_{ph}}{\eta_{ph}+\beta_\Gamma}$ as in item 2.

4. If we use the approximations in §2.4 to derive equation 13 of BMS97 from equation 9 of that same work, we find three differences between our calculation and their equation 13: the factor of π^5 should be π^4, there is an extra factor of R in the numerator, and their expression is too large by a factor of 2 (the 40 in the denominator should be 80). Because of the last error, our expression (equation 39) is larger than their equation 13

by a factor of 2, not 4, as in the previous expressions for the loss rate. Also, their equation 13 omits the factor of $\frac{1+\beta_\Gamma \eta_{ph}}{\eta_{ph}+\beta_\Gamma}$, just as in their equations 9 and 12.

2.6. Emitted inverse-Compton spectrum

In this section we derive an expression for the photon spectrum that results from inverse-Compton scattering of accretion disk photons off of the jet blob. Following equation 49 of BMS97, we set up the photon spectrum equation in the blob frame:

$$\begin{aligned} \frac{d^2\dot{n}_{ECD}}{d\epsilon_s d\Omega_{ph,s}} &= c\int_0^\infty d\epsilon \int_{4\pi} d\widetilde{\Omega}_{ph}\, \frac{d^2 n_{ph}}{d\epsilon d\widetilde{\Omega}_{ph}} \int_1^\infty d\gamma \\ &\times \int_{4\pi} d\Omega_e\, \frac{d^2 n_e(\gamma)}{d\gamma d\Omega_e}\,(1-\beta\mu)\,\frac{d^2\sigma_{KN}}{d\epsilon_s d\Omega_{ph,s}}\ , \end{aligned} \tag{42}$$

where $\Omega_{ph,s} = (\mu_s, \alpha_s)$, $\widetilde{\Omega}_{ph} = (\eta_{ph}, \phi_{ph})$, and $\Omega_e = (\eta_e, \phi_e)$ are the solid angle directions of the scattered photon, incoming photon, and electron, respectively; $\phi = \phi_{ph} - \phi_e$; and the angles are defined by equation 1 and pictured in Figure 2. Note that this is a different definition of $\Omega_{ph,s}$ than that used in equation 10, one more convenient to the geometry considered here. Also, the definition of $\widetilde{\Omega}_{ph}$ is slightly different from Ω_{ph}: ϕ_{ph} is used as the azimuthal angle instead of ϕ, since the latter is defined with respect to the electron direction of motion, and here we are integrating over different electron directions. The factor $\frac{d^2 n_{ph}}{d\epsilon d\widetilde{\Omega}_{ph}}$ is the accretion disk flux from equation 9, and $\frac{d^2 n_e(\gamma)}{d\gamma d\Omega_e}$ is the electron density in particles sr^{-1} per unit Lorentz factor. As in equation 10, $c(1-\beta\mu)$ is the relative velocity between the relativistic electron and the photon. In equation 42, we integrate over all incoming photon directions and energies and over all electron directions and energies.

We are interested in evaluating equation 42 in the direction of the observer:

$$\frac{d^2\dot{n}_{ECD}}{d\epsilon_s d\Omega_{obs}} = \int_{4\pi} d\Omega_{ph,s} \frac{d^2\dot{n}_{ECD}}{d\epsilon_s d\Omega_{ph,s}}\bigg|_{\substack{\alpha_s=\alpha_{obs}\\ \mu_s=\mu_{obs}}} \tag{43}$$

where the observing angles μ_{obs} and α_{obs} are defined in the blob frame. We can relate μ_{obs} and α_{obs} to the usual observing angles, η^*_{obs} and ϕ^*_{obs}. First, from equation 1c, we have

$$\mu_{obs} = \eta_{obs}\eta_e + \sin\theta_{obs}\sin\theta_e\cos\phi_{obs} \ . \tag{44}$$

Due to the azimuthal symmetry of the jet, we are free to choose ϕ_{obs}. Setting $\phi_{obs} = \frac{\pi}{2}$ simplifies equation 44, giving

$$\mu_{obs} = \eta_{obs}\eta_e \ . \tag{45}$$

Then, from equation A2,

$$\eta_{obs} = \frac{\eta^*_{obs} - \beta_\Gamma}{1 - \beta_\Gamma\eta^*_{obs}} \ . \tag{46}$$

We can also express α_{obs} in terms of η_{obs} (see Figure 2, bottom),

$$\cos\alpha_{obs} = \frac{\eta_{obs} - \eta_e\mu_{obs}}{\sqrt{(1-\eta_e^2)(1-\mu_{obs}^2)}} \ , \tag{47}$$

although this is not needed in equation 43.

$\frac{d^2\sigma_{KN}}{d\epsilon_s d\Omega_{ph,s}}$ is the Klein-Nishina scattering cross section in the blob frame. It is usually given in the electron rest frame, and we transform to the blob frame with

$$\frac{d^2\sigma_{KN}}{d\epsilon_s d\Omega_{ph,s}} = \frac{d^2\sigma_{KN}}{d\epsilon'_s d\Omega'_{ph,s}}\frac{d\epsilon'_s}{d\epsilon_s}\frac{d\mu'_s}{d\mu_s}\frac{d\alpha'_s}{d\alpha_s} \ , \tag{48}$$

where $\frac{d^2\sigma_{KN}}{d\epsilon'_s d\Omega'_{ph,s}}$ is given by equation 12. From equation A1,

$$\epsilon'_s = \frac{\epsilon_s(1-\beta\mu_s)}{\sqrt{1-\beta^2}} = \epsilon_s\gamma(1-\beta\mu_s) \ , \tag{49}$$

so

$$\frac{d\epsilon'_s}{d\epsilon_s} = \gamma(1-\beta\mu_s) \ . \tag{50}$$

Likewise, from equation A2,

$$\mu'_s = \frac{\mu_s - \beta}{1-\beta\mu_s} \ , \tag{51}$$

so

$$\frac{d\mu_s'}{d\mu_s} = \frac{1}{\gamma(1-\beta\mu_s)^2} \ . \tag{52}$$

Because α_s is defined about the direction of motion of the electron,

$$\frac{d\alpha_s'}{d\alpha_s} = 1 \ . \tag{53}$$

Plugging equations 12, 16, 49, 50, 52, and 53 into 48, we have

$$\begin{aligned} \frac{d^2\sigma_{KN}}{d\epsilon_s d\Omega_{ph,s}} &= \frac{r_e^2}{2}\left(\frac{\epsilon_s(1-\beta\mu_s)}{\epsilon(1-\beta\mu)}\right)^2 \frac{1}{\gamma(1-\beta\mu_s)}\left(\frac{\epsilon(1-\beta\mu)}{\epsilon_s(1-\beta\mu_s)} + \frac{\epsilon_s(1-\beta\mu_s)}{\epsilon(1-\beta\mu)} - \sin^2\chi'\right) \\ &\times \ \delta\left(\epsilon_s\gamma(1-\beta\mu_s) - \frac{\epsilon\gamma(1-\beta\mu)}{1+\epsilon\gamma(1-\beta\mu)(1-\kappa')}\right) \ . \end{aligned} \tag{54}$$

We can also express κ in terms of κ' by taking the scalar product of the four-momentum of the incoming and scattered photons, a Lorentz invariant quantity, giving

$$\epsilon_s\epsilon(1-\kappa) = \epsilon_s'\epsilon'(1-\kappa') \ , \tag{55}$$

or, with equations 16 and 49,

$$1-\kappa' = \frac{1-\kappa}{\gamma^2(1-\beta\mu_s)(1-\beta\mu)} \tag{56}$$

(*cf.* equation 51 of BMS97).

We can rewrite the delta function in equation 54 with

$$\delta(f(\epsilon_s)) = \sum_i \frac{\delta(\epsilon_s - \epsilon_{s,i})}{|f'(\epsilon_{s,i})|} \ , \tag{57}$$

where

$$\begin{aligned} f(\epsilon_s) &= \epsilon_s\gamma(1-\beta\mu_s) - \frac{\epsilon\gamma(1-\beta\mu)}{1+\epsilon\gamma(1-\beta\mu)(1-\kappa')} \ , \\ f'(\epsilon_{s,i}) &= \gamma(1-\beta\mu_s) \ , \end{aligned} \tag{58}$$

and i refers to the roots of $f(\epsilon_s)$. Using equation 56 for $1-\kappa'$, we find

$$\epsilon_{s,i} = \frac{\epsilon\gamma(1-\beta\mu)}{\epsilon(1-\kappa)+\gamma(1-\beta\mu_s)} \ . \tag{59}$$

After recasting the delta function, the final expression for the full Klein-Nishina cross section in the blob frame is

$$\begin{aligned}\frac{d^2\sigma_{KN}}{d\epsilon_s^2 d\Omega_{ph,s}} &= \frac{r_e^2}{2\gamma^2}\left(\frac{\epsilon_s}{\epsilon}\right)^2 \frac{1}{(1-\beta\mu)^2}\left(\frac{\epsilon(1-\beta\mu)}{\epsilon_s(1-\beta\mu_s)}+\frac{\epsilon_s(1-\beta\mu_s)}{\epsilon(1-\beta\mu)}-\sin\chi'^2\right) \\ &\times \delta\left(\epsilon_s-\frac{\epsilon\gamma(1-\beta\mu)}{\epsilon(1-\kappa)+\gamma(1-\beta\mu_s)}\right) \end{aligned} \tag{60}$$

(*cf.* equation 50 of BMS97), where $\sin\chi' = \sqrt{1-\kappa'^2}$ is found from equation 56 and

$$\kappa = \eta_{ph}\eta_{ph,s} + \sqrt{(1-\eta_{ph}^2)(1-\eta_{ph,s}^2)}\cos(\phi-\phi_s) \tag{61}$$

(see Figure 2e).

We can substitute equation 60 for the cross section into equation 42, giving for equation 43:

$$\begin{aligned}\frac{d^2\dot{n}_{ECD}}{d\epsilon_s d\Omega_{obs}} &= \left[\frac{cr_e^2}{2}\int_0^\infty d\epsilon \int_{4\pi} d\widetilde{\Omega}_{ph}\frac{d^2n_{ph}}{d\epsilon d\widetilde{\Omega}_{ph}}\int_1^\infty \frac{d\gamma}{\gamma^2}\int_{4\pi} d\Omega_e \frac{d^2n_e(\gamma)}{d\gamma d\Omega_e}\frac{1}{1-\beta\mu}\right. \\ &\times \left(\frac{\epsilon_s}{\epsilon}\right)^2\left(\frac{\epsilon(1-\beta\mu)}{\epsilon_s(1-\beta\mu_s)}+\frac{\epsilon_s(1-\beta\mu_s)}{\epsilon(1-\beta\mu)}-\sin\chi'^2\right) \\ &\times \left.\delta\left(\epsilon_s-\frac{\epsilon\gamma(1-\beta\mu)}{\epsilon(1-\kappa)+\gamma(1-\beta\mu_s)}\right)\right]_{\substack{\alpha_s=\alpha_{obs}\\ \mu_s=\mu_{obs}}} . \end{aligned} \tag{62}$$

The full expression for the disk flux $\frac{d^2n_{ph}}{d\epsilon d\widetilde{\Omega}_{ph}}$ is given by equation 9. However, it is convenient to use a delta-function approximation for this flux instead, as we did in §2.4. Then,

$$\frac{\epsilon^2}{e^{\frac{\epsilon\Gamma(1+\beta_\Gamma\eta_{ph})}{\Theta(R)}}-1} \rightarrow B\delta(\epsilon - <\epsilon>) , \tag{63}$$

where

$$B = \int_0^\infty d\epsilon \frac{\epsilon^2}{e^{\frac{\epsilon\Gamma(1+\beta_\Gamma\eta_{ph})}{\Theta(R)}}-1} = \Gamma(3)\zeta(3)\left[\frac{\Theta(R(\eta_{ph}))}{\Gamma(1+\beta_\Gamma\eta_{ph})}\right]^3 \tag{64}$$

and $<\epsilon>$ is given by equation 36. Substituting equation 63 into equation 62, integrating over ϵ, and evaluating μ_s and α_s, we have

$$\frac{d^2\dot{n}_{ECD}}{d\epsilon_s d\Omega_{obs}} = \frac{r_e^2}{c^2}\frac{\Gamma(3)\zeta(3)}{\Gamma^3}\left(\frac{m_e c^2}{h}\right)^3\int_1^\infty\frac{d\gamma}{\gamma^2}\int_{4\pi} d\widetilde{\Omega}_{ph}\left[\frac{\Theta(R(\eta_{ph}))}{1+\beta_\Gamma\eta_{ph}}\right]^3\frac{1}{1-\beta\mu}$$

$$\times \int_{4\pi} d\Omega_e \frac{d^2 n_e(\gamma)}{d\gamma d\Omega_e} \left(\frac{\epsilon_s}{<\epsilon>}\right)^2 \left(\frac{<\epsilon>(1-\beta\mu)}{\epsilon_s(1-\beta\mu_{obs})} + \frac{\epsilon_s(1-\beta\mu_{obs})}{<\epsilon>(1-\beta\mu)} - \sin\chi'^2\right)$$
$$\times \delta\left(\epsilon_s - \frac{<\epsilon>\gamma(1-\beta\mu)}{<\epsilon>(1-\kappa)+\gamma(1-\beta\mu_{obs})}\right) , \quad (65)$$

where

$$\kappa = \eta_{ph}\eta_{obs} + \sqrt{(1-\eta_{ph}^2)(1-\eta_{obs}^2)}\cos\left(\phi - \frac{\pi}{2}\right) , \quad (66)$$

μ_{obs} is given by equation 45, and μ is given by equation 1c.

We can use the delta function in equation 65 to integrate over η_e, using

$$\delta(f(\eta_e)) = \sum_i \frac{\delta(\eta_e - \eta_{e,i})}{|f'(\eta_{e,i})|} \quad (67)$$

and

$$\begin{aligned} f(\eta_e) &= \epsilon_s - \frac{<\epsilon>\gamma(1-\beta\mu)}{<\epsilon>(1-\kappa)+\gamma(1-\beta\mu_{obs})} \\ &= \epsilon_s - \frac{<\epsilon>\gamma(1-\beta\eta_{ph}\eta_e - \beta\sqrt{(1-\eta_{ph}^2)(1-\eta_e^2)}\cos\phi)}{<\epsilon>(1-\kappa)+\gamma(1-\beta\eta_{obs}\eta_e)} . \end{aligned} \quad (68)$$

Solving for η_e, there are two solutions,

$$\eta_{e,1} = \frac{q}{a} \quad \text{and} \quad \eta_{e,2} = \frac{c}{q} , \quad (69)$$

where

$$q \equiv -\frac{1}{2}(b + \mathrm{sgn}(b)\sqrt{b^2 - 4ac}) , \quad (70)$$

$$a = <\epsilon>^2 \gamma^2\beta^2(1-\eta_{ph}^2)\cos\phi^2 + \gamma^2\beta^2(<\epsilon>\eta_{ph} - \epsilon_s\eta_{obs})^2 , \quad (71)$$

$$b = 2[\epsilon_s <\epsilon>(1-\kappa) + \gamma(\epsilon_s - <\epsilon>)][\gamma\beta(<\epsilon>\eta_{ph} - \epsilon_s\eta_{obs})] , \quad (72)$$

$$c = [\epsilon_s <\epsilon>(1-\kappa) + \gamma(\epsilon_s - <\epsilon>)]^2 - <\epsilon>^2 \gamma^2\beta^2(1-\eta_{ph}^2)\cos^2\phi . \quad (73)$$

Also,

$$\frac{df}{d\eta_e} = \frac{<\epsilon>\gamma\beta\frac{d\mu}{d\eta_e}[<\epsilon>(1-\kappa)+\gamma(1-\beta\eta_{obs}\eta_e)] - <\epsilon>\gamma^2\beta\eta_{obs}(1-\beta\mu)}{[<\epsilon>(1-\kappa)+\gamma(1-\beta\eta_{obs}\eta_e)]^2} \quad (74)$$

and

$$\frac{d\mu}{d\eta_e} = \eta_{ph} - \eta_e \cos\phi \sqrt{\frac{1-\eta_{ph}^2}{1-\eta_e^2}} \ . \tag{75}$$

With equation 67, we can evaluate the integral over η_e. If we assume azimuthal symmetry in the electron population, so that n_e is not a function of ϕ_e, then the integrals over the azimuthal angles ϕ_{ph} and ϕ_e only enter as the difference $\phi = \phi_{ph} - \phi_e$. Therefore, we can choose $\phi_e = 0$, yielding a factor of 2π for the integral over ϕ_e. This leaves a final expression with three integrals to be performed numerically, over η_{ph}, ϕ_{ph}, and γ. The final expression for the spectrum due to external inverse-Compton scattering of direct disk emission is

$$\begin{aligned}
\frac{d^2\dot{n}_{ECD}}{d\epsilon_s d\Omega_{obs}} &= \frac{2\pi r_e^2}{c^2} \frac{\Gamma(3)\zeta(3)}{\Gamma^3} \left(\frac{m_e c^2}{h}\right)^3 \int_1^\infty \frac{d\gamma}{\gamma^2} \int_0^{2\pi} d\phi_{ph} \int_{\eta_{ph,min}}^{\eta_{ph,max}} d\eta_{ph} \left[\frac{\Theta(R(\eta_{ph}))}{1+\beta_\Gamma \eta_{ph}}\right]^3 \\
&\times \left(\frac{\epsilon_s}{<\epsilon>}\right)^2 \sum_i \frac{1}{1-\beta\mu_i} \left[\frac{d^2 n_e(\gamma)}{d\gamma d\eta_e}\right]_{\eta_e=\eta_{e,i}} \frac{1}{|f'(\eta_{e,i})|} \\
&\times \left(\frac{<\epsilon>(1-\beta\mu_i)}{\epsilon_s(1-\beta\mu_{obs})} + \frac{\epsilon_s(1-\beta\mu_{obs})}{<\epsilon>(1-\beta\mu_i)} - \sin\chi'^2\right) \ ,
\end{aligned} \tag{76}$$

where

$$\mu_i = \eta_{ph}\eta_{e,i} + \sqrt{(1-\eta_{ph}^2)(1-\eta_{e,i}^2)}\cos\phi_{ph} \ , \tag{77}$$

$$\sin\chi' = \sqrt{1-\kappa'^2} \ , \tag{78}$$

$$\kappa = \eta_{ph}\eta_{obs} + \sqrt{(1-\eta_{ph}^2)(1-\eta_{obs}^2)}\cos\left(\phi_{ph} - \frac{\pi}{2}\right) \ , \tag{79}$$

and we use R_{min} and R_{max} in equation 22 to find the limits of integration of η_{ph}, $\eta_{ph,min}$ and $\eta_{ph,max}$.

2.7. Thomson limit for the emitted spectrum

In the regime of low electron energies, $\gamma\epsilon \ll 1$, we can use the Thomson cross section σ_T instead of the full Klein-Nishina cross section given in equation 60:

$$\frac{d^2\sigma_{Th}}{d\epsilon_s d\Omega_{ph,s}} = \frac{\sigma_T}{4\pi}\delta\left(\epsilon_s - \frac{\epsilon\gamma(1-\beta\mu)}{\epsilon(1-\kappa)+\gamma(1-\beta\mu_s)}\right) \ . \tag{80}$$

Substituting this expression into equation 42, we have

$$\begin{aligned}\frac{d^2\dot{n}_{ECD,Thomson}}{d\epsilon_s d\Omega_{obs}} &= \left[\frac{c\sigma_T}{4\pi}\int_0^\infty d\epsilon \int_{4\pi} d\widetilde{\Omega}_{ph}\,\frac{d^2n_{ph}}{d\epsilon d\widetilde{\Omega}_{ph}}\int_1^\infty d\gamma\int_{4\pi} d\Omega_e\,\frac{dn_e(\gamma)}{d\Omega_e}\,(1-\beta\mu)\right. \\ &\times \left.\delta\left(\epsilon_s - \frac{\epsilon\gamma(1-\beta\mu)}{\epsilon(1-\kappa)+\gamma(1-\beta\mu_s)}\right)\right]_{\substack{\alpha_s=\alpha_{obs}\\ \mu_s=\mu_{obs}}}\end{aligned} \tag{81}$$

(*cf.* equation 62). Again using a delta-function approximation for the accretion disk flux (equations 63 and 64), rewriting the delta function in equation 81 in terms of η_e, and integrating over η_e and ϕ_e, we have

$$\begin{aligned}\frac{d^2\dot{n}_{ECD,Thomson}}{d\epsilon_s d\Omega_{obs}} &= \frac{\sigma_T\Gamma(3)\zeta(3)}{c^2\Gamma^3}\left(\frac{m_e c^2}{h}\right)^3\int_1^\infty d\gamma\int_0^{2\pi} d\phi_{ph}\int_{\eta_{ph,min}}^{\eta_{ph,max}} d\eta_{ph}\left[\frac{\Theta(R(\eta_{ph}))}{1+\beta_\Gamma\eta_{ph}}\right]^3 \\ &\times \sum_i \frac{(1-\beta\mu_i)n_{e,i}(\gamma)}{|f'(n_{e,i})|} \ ,\end{aligned} \tag{82}$$

where μ_i, κ', and κ are given by equations 77, 78, and 79, respectively.

3. External inverse-Compton scattering of BLR-scattered photons

This section introduces the equations describing the external inverse-Compton scattering of seed photons that originated from the accretion disk and scattered off the broad line region (BLR) ("external Compton from clouds", or ECC). As in the previous section, we first derive an expression for the seed photon spectrum encountered by the jet blob (§3.1 and §3.2). Then we derive expressions for the single electron energy loss rate (§3.3) and the inverse-Compton radiation spectrum (§3.4).

3.1. Seed photon flux at jet

Here we derive an expression for the differential photon flux incident on the blob, $\frac{d^2 n_{ph}}{d\epsilon d\Omega_{ph}}$, in the frame of the accretion disk. This is an expansion of the description in §2 of Böttcher and Dermer (1995). The steps below follow the photons as they leave the accretion disk, scatter off the BLR, and enter the jet blob. These steps are labeled in Figure 3.

1. Let the differential accretion disk photon flux per unit energy and solid angle be $\frac{d^2 \dot{N}_D}{d\epsilon d\Omega_D}$, where $\Omega_D = (\eta_D, \phi_D)$ is the solid angle of emission of accretion disk photons with respect to the jet axis, in the disk frame, as shown in Figure 3. For now, we omit the asterisks on the angles.

2. The disk flux into solid angle $d\Omega_D$ incident on a BLR scattering site of differential area dA located a distance r from the accretion disk is

$$\left(\frac{d^2 \dot{n}_{ph}}{d\epsilon d\Omega_D}\right)_{in} = \frac{\frac{d^2 \dot{N}_D}{d\epsilon d\Omega_D} d\Omega_D}{r^2 d\Omega_D} \ . \tag{83}$$

If we consider a differential volume element $dV = dr \times dA$ at the scattering site, then the photon density in that volume is

$$\begin{aligned} \left(\frac{d^2 n_{ph}}{d\epsilon d\Omega_D}\right)_{in} &= c^{-1} \int \left(\frac{d^2 \dot{n}_{ph}}{d\epsilon d\Omega_D}\right)_{in} \delta(\eta_D - \bar{\eta}_D)\, \delta(\phi_D - \bar{\phi}_D)\, \delta(\epsilon - \epsilon_s)\, d\Omega_D\, d\epsilon\, dt \\ &= \frac{1}{r^2 c} \frac{d^2 \dot{N}_D}{d\epsilon_s d\bar{\Omega}_D} \ , \end{aligned} \tag{84}$$

where ϵ_s is the BLR-scattered photon energy[2]. For Thomson scattering, $\epsilon_s = \epsilon$.

[2]Böttcher and Dermer (1995) include a delta function in time, $\delta\left(t - \left(t_0 - \frac{r}{c}\right)\right)$, to account for the time delay between emission at the disk and scattering at the BLR. Here we assume steady disk emission.

3. The scattering rate for each photon is

$$r_s = \sigma(\epsilon)\, n_{blr}(\vec{r}) c \ , \tag{85}$$

where $\sigma(\epsilon)$ is the cross section and $n_{blr}(\vec{r})$ is the BLR electron density at $\vec{r}$. For Thomson scattering, $\sigma(\epsilon) = \sigma_T$. The scattered photon flux density at $\vec{r}$ is

$$\begin{aligned} \left(\frac{d^2\dot{n}_{ph}}{d\epsilon d\Omega_D}\right)_{out} &= \left(\frac{d^2 n_{ph}}{d\epsilon d\Omega_D}\right)_{in} \times r_s \times \frac{1}{4\pi} \\ &= \frac{1}{4\pi r^2}\, \frac{d^2\dot{N}_D}{d\epsilon_s d\bar{\Omega}_D}\, \sigma(\epsilon)\, n_{blr}(\vec{r}) \ , \end{aligned} \tag{86}$$

where the division by 4π arises from the assumption of isotropic scattering.

4. We are interested in the scattered flux density incident on a single point in the blob, a distance $d = \sqrt{r^2 + z^2 - 2rz\eta_D^*}$ from the BLR scattering site and z from the accretion disk, where $\eta_D^* = \cos\theta_D^*$ (see Figure 3). The scattered photon flux density from a differential scattering site at $\vec{r}$, $\left(\frac{d^2\dot{n}_{ph}}{d\epsilon d\Omega_D}\right)_{out}$, contributes a flux density $\left(\frac{d^2\dot{n}_{ph}}{d\epsilon d\Omega_D}\right)_{out} \times \frac{1}{cd^2}$ at d. We integrate this over all space to find the total scattered flux density at d:

$$\begin{aligned} \left(\frac{dn_{ph}}{d\epsilon}\right)^* &= \int_{4\pi} d\Omega_D^* \int_0^\infty r^2\, dr\, \frac{1}{cd^2} \left(\frac{d^2\dot{n}_{ph}}{d\epsilon d\Omega_D}\right)^*_{out} \\ &= \frac{\sigma_T}{4\pi c} \int_{4\pi} d\Omega_D^* \int_0^\infty dr\, \left(\frac{d^2\dot{N}_D}{d\epsilon_s d\bar{\Omega}_D}\right)^* \frac{n_{blr}(\vec{r})}{d^2} \ . \end{aligned} \tag{87}$$

Here we have added the asterisks to emphasize that this expression applies to the disk frame.

To complete the expression, we add the delta-function dependence on the scattering angles, since we are only interested in the flux at a single point in the jet:

$$\left(\frac{d^2 n_{ph}}{d\epsilon d\Omega_{ph}}\right)^* = \frac{\sigma_T}{4\pi c} \int_{4\pi} d\Omega_D^* \int_{r_{in}}^{r_{out}} dr\, \left(\frac{d^2\dot{N}_D}{d\epsilon_s d\bar{\Omega}_D}\right)^* \frac{n_{blr}(\vec{r})}{d^2}\, \delta(\phi^* - \bar{\phi}^*)\, \delta(\eta_{ph}^* - \bar{\eta}_{ph}^*) \ , \tag{88}$$

where

$$\bar{\eta}_{ph}^* = \sqrt{1 - \left(\frac{r}{d}\right)^2 (1 - \eta_D^{*2})} \tag{89}$$

and

$$\bar{\phi}^* = \pi + \phi_D^* \tag{90}$$

(*cf.* equation 8 of Böttcher and Dermer (1995)).We have also limited the integration over r to (r_{in}, r_{out}), the inner and outer radius of the BLR. This is the final expression for the photon flux at the jet blob from disk photons scattered off of the BLR; it is comparable to equation 8 for the direct disk emission.

3.2. Approximation of the accretion disk spectrum

The treatment of accretion disk emission incident directly on the jet in §2 considered a profile for the accretion disk in which its blackbody temperature varies as a function of radius. Here, we approximate the accretion disk as a point source radiating isotropically, in keeping with the Appendix of Böttcher and Bloom (2000). This is valid since the disk emission originates from within a radius much smaller than the BLR size scales we consider. We find a blackbody-like spectrum by integrating equation 8 over R; the peak of this spectrum represents the characteristic temperature of the disk, Θ_D. Then, the photon flux from the disk is

$$\left(\frac{d^2\dot{N}_D}{d\epsilon d\Omega_D}\right)^* = \frac{K}{4\pi}\frac{\epsilon^{*2}}{e^{\frac{\epsilon^*}{\Theta_D}}-1} \ , \tag{91}$$

where we relate K to the disk luminosity L_D by integrating the energy spectrum over all energies:

$$L_D = m_e c^2 \int_0^\infty d\epsilon^* \int_{4\pi} d\Omega_D \, \epsilon^* \left(\frac{d^2\dot{N}_D}{d\epsilon d\Omega_D}\right)^* = K m_e c^2 \frac{\pi^4}{15}\Theta_D^4 \ . \tag{92}$$

Note that since the disk is optically thick, the photon flux available to each jet is *half* of the total flux. If L_D is the total measured disk luminosity, then we should divide it in half to correctly normalize $\left(\frac{d^2\dot{N}_D}{d\epsilon d\Omega_D}\right)^*$. Solving equation 92 and including this correction,

$$K = \frac{L_D}{2m_e c^2}\frac{15}{\pi^4\Theta_D^4} \ . \tag{93}$$

Plugging equation 91 for the accretion disk emission into equation 88, we have

$$\left(\frac{d^2n_{ph}}{d\epsilon d\Omega_{ph}}\right)^* = \frac{\sigma_T}{4\pi c}\frac{K}{4\pi}\int_{4\pi} d\Omega_D^* \frac{\epsilon^{*2}}{e^{\frac{\epsilon^*}{\Theta_D}}-1}\int_{r_{in}}^{r_{out}} dr \frac{n_{blr}(\vec{r})}{d^2}\,\delta(\phi^*-\bar{\phi}^*)\,\delta(\eta_{ph}^*-\bar{\eta}_{ph}^*)\ . \tag{94}$$

We convert the integral over $d\Omega_D^*$ to an integral over $d\Omega_{ph}^*$ with equation 89,

$$d\eta_{ph}^* = \frac{\partial\eta_{ph}^*}{\partial\eta_D^*}d\eta_D^*\ , \tag{95}$$

$$\frac{\partial\eta_{ph}^*}{\partial\eta_D^*} = \frac{r^2[\eta_D^* d^2 - rz(1-\eta_D^{*2})]}{d^3\sqrt{d^2-r^2(1-\eta_D^{*2})}} = \frac{r^2(\eta_D^* r - z)(r-\eta_D^* z)}{d^3|\eta_D^* r - z|} = \frac{r^2|r-\eta_D^* z|}{d^3}\ , \tag{96}$$

and

$$\frac{1}{d^2}\frac{\partial\eta_D^*}{\partial\eta_{ph}^*} = \frac{d}{r^2|r-\eta_D^* z|}\ . \tag{97}$$

Integrating over $d\Omega_{ph}^*$, the photon flux incident on the blob is

$$\left(\frac{d^2n_{ph}}{d\epsilon d\bar{\Omega}_{ph}}\right)^* = \frac{\sigma_T K}{16\pi^2 c}\frac{\epsilon^{*2}}{e^{\frac{\epsilon^*}{\Theta_D}}-1}\int_{r_{in}}^{r_{out}} dr\frac{n_{blr}(\vec{r})d}{r^2|r-\eta_D^* z|}\ . \tag{98}$$

Note that this is equivalent to the expression in equation A3 of (Böttcher and Bloom 2000), since

$$\frac{d}{r|z^2-d^2-rz\eta_D^*|} = \frac{d}{r^2|r-\eta_D^* z|}\ . \tag{99}$$

We convert equation 98 to the rest frame of the blob using the two equations from appendix A:

$$\epsilon^* = \epsilon\Gamma(1+\beta_\Gamma\eta_{ph})\ , \tag{100}$$

and

$$\eta_{ph}^* = \frac{\eta_{ph}+\beta_\Gamma}{1+\beta_\Gamma\eta_{ph}}\ , \tag{101}$$

where $\eta_{ph}^* = \cos\theta_{ph}^*$ and θ_{ph}^* is the angle between $\vec{d}$ and $\hat{z}$, as shown in Figure 3. As in equation 9, we invoke Lorentz invarience and find

$$\frac{d^2n_{ph}}{d\epsilon d\bar{\Omega}_{ph}} = \left(\frac{\epsilon}{\epsilon^*}\right)^2\left(\frac{d^2n_{ph}}{d\epsilon d\bar{\Omega}_{ph}}\right)^* = \frac{\sigma_T K}{16\pi^2 c}\frac{\epsilon^2}{e^{\frac{\epsilon\Gamma(1+\beta_\Gamma\eta_{ph})}{\Theta_D}}-1}\int_{r_{in}}^{r_{out}} dr\frac{n_{blr}(\vec{r})d}{r^2|r-\eta_D^* z|}\ . \tag{102}$$

Finally, we solve equation 89 for η_D^*:

$$\eta_{ph}^* = \sqrt{1 - \left(\frac{r}{d}\right)^2 (1 - \eta_D^{*2})} = \sqrt{\frac{z^2 - 2rz\eta_D^* + r^2\eta_D^{*2}}{r^2 + z^2 - 2rz\eta_D^*}} \ , \tag{103}$$

and

$$\eta_D^* = \frac{z}{r}(1 - \eta_{ph}^{*2}) \pm \sqrt{1 - \left(\frac{z}{r}\right)^2 (1 - \eta_{ph}^{*2})} \ . \tag{104}$$

Equation 102 is the final expression for the seed photon flux in the blob frame, equivalent to equation 9 for ECD scattering.

3.3. Single electron energy loss

We now calculate the single electron energy loss in a manner similar to the derivation in §2. Using equation 102 for the photon flux in equation 21, we have

$$\begin{aligned} -\left(\frac{d\gamma}{dt}\right)_{ECC} &= \frac{c\pi r_e^2}{2}\frac{\sigma_T K}{16\pi^2 c}\int_{-1}^{1} d\eta_e \int_{-1}^{1} d\eta_{ph} \int_0^{2\pi} d\phi \int_0^{\infty} d\epsilon \int_{-1}^{1} d\kappa'(1 - \beta\mu)\frac{\epsilon^2}{e^{\frac{\epsilon\Gamma(1+\beta_\Gamma\eta_{ph})}{\Theta_D}} - 1} \\ &\times \ \epsilon\left(\frac{1 + F\kappa'^2 + F(F-1)}{F^3}\right)\left(\frac{\gamma^2[1 - \beta\mu + \beta\kappa'(\mu - \beta)]}{F} - 1\right) \\ &\times \ \int_{r_{in}}^{r_{out}} dr \frac{n_{blr}(\vec{r})d}{r^2|r - \eta_D^* z|} \ . \end{aligned} \tag{105}$$

From here, we can make the same approximations made in §2.4. First, we let

$$\frac{\epsilon^3}{e^{\frac{\epsilon\Gamma(1+\beta_\Gamma\mu)}{\Theta_D}} - 1} \rightarrow A\delta(\epsilon - < \epsilon >) \ , \tag{106}$$

as in equation 33, where A and $< \epsilon >$ are given by equations 34 and 36, respectively, except that $\Theta(R) \rightarrow \Theta_D$, which is no longer a function of disk radius. Second, we neglect terms of order $\left(\frac{1}{\gamma^2}\right)$, as in equation 37. Finally, we replace the integral over η_e that averages over all electron directions by setting $\eta_e = 0$. With these approximations, the single electron energy loss rate from BLR-scattered photons is

$$-\left(\frac{d\gamma}{dt}\right)_{ECC} = \frac{\pi^3 r_e^2 \sigma_T K \Theta_D^4}{240\Gamma^4}\gamma^2 \int_{-1}^{1} \frac{d\eta_{ph}}{(1 + \beta_\Gamma\eta_{ph})^4} I(< \epsilon >, \gamma, \eta_{ph}) \int_{r_{in}}^{r_{out}} dr \frac{n_{blr}(\vec{r})d}{r^2|r - \eta_D^* z|} \ , \tag{107}$$

where I is given by equation 40 and $\eta_D^* = \eta_D^*(\eta_{ph}, \Gamma, z, r)$ is given by equations 101 and 104.

Equation 107 assumes a spherical geometry for the BLR (labeled 'BLR' in Figure 1). Since η_D^* is integrated over all space, from -1 to 1, η_{ph} is also integrated over all space. However, in the disk wind geometry, with $\theta_{wind} \neq 0$, the limits of η_{ph} depend on r and θ_{wind}. Therefore, the integrals in equations 105 and 107 must be rearranged. Since $\eta_{ph,min}$ and $\eta_{ph,max}$ depend on r, we set the integral over η_{ph} as the innermost one, yielding the more general expression:

$$-\left(\frac{d\gamma}{dt}\right)_{ECC} = \frac{\pi^3 r_e^2 \sigma_T K \Theta_D^4}{240\Gamma^4}\gamma^2 \int_{r_{in}}^{r_{out}} dr \frac{n_{blr}(\vec{r})d}{r^2|r - \eta_D^* z|} \int_{\eta_{ph,min}}^{\eta_{ph,max}} \frac{d\eta_{ph}}{(1+\beta_\Gamma \eta_{ph})^4} I(<\epsilon>, \gamma, \eta_{ph}) \ , \tag{108}$$

where $\eta_{ph,max}^* = \sqrt{1 - \left(\frac{r}{d}\right)^2 (1 - \cos\theta_{wind})}$, and $\eta_{ph,min}^* = 1$. In these expressions, we have assumed that the lower boundary of the disk wind runs along the x-axis, as defined in Figure 1. However, this is easily generalized, and the code allows for arbitrary upper and lower bounds on η_D^*.

3.4. Emitted inverse-Compton spectrum

Finally, we derive an expression for the inverse-Compton spectrum emitted by the jet blob due to BLR-scattered photons. We begin from equation 62 for the photon spectrum ($\frac{d^2\dot{n}_{ECC}}{d\epsilon_s d\Omega_{obs}}$), and we use equation 102 for the seed photon flux at the blob ($\frac{d^2 n_{ph}}{d\epsilon d\Omega_{ph}}$). We also approximate the exponential in equation 102 as we have before, using the delta-function approximation in equations 36, 63, and 64. After integrating over ϵ and evaluating μ_s and α_s, we have

$$\frac{d^2\dot{n}_{ECC}}{d\epsilon_s d\Omega_{obs}} = \frac{r_e^2 \sigma_T K}{32\pi^2} \frac{\Gamma(3)\zeta(3)}{\Gamma^3} \int_1^\infty \frac{d\gamma}{\gamma^2} \int_{4\pi} d\Omega_{ph} \left[\frac{\Theta_D}{1+\beta_\Gamma \eta_{ph}}\right]^3 \frac{1}{1-\beta\mu}$$

$$\times \int_{4\pi} d\Omega_e \frac{dn_e(\gamma)}{d\Omega_e} \left(\frac{\epsilon_s}{<\epsilon>}\right)^2 \left(\frac{<\epsilon>(1-\beta\mu)}{\epsilon_s(1-\beta\mu_{obs})} + \frac{\epsilon_s(1-\beta\mu_{obs})}{<\epsilon>(1-\beta\mu)} - \sin\chi'^2\right)$$
$$\times \delta\left(\epsilon_s - \frac{<\epsilon>\gamma(1-\beta\mu)}{<\epsilon>(1-\kappa)+\gamma(1-\beta\mu_{obs})}\right)$$
$$\times \int_{r_{in}}^{r_{out}} dr \frac{n_{blr}(\vec{r})d}{r^2|r-\eta_D^* z|} \ . \tag{109}$$

This differs from equation 65 only in the constant factors and in the integration over r.

As in §2.6, we utilize the delta function in equation 109 to integrate over η_e, and we integrate over ϕ_e assuming that n_e is not a function of ϕ_e. Then we have

$$\frac{d^2\dot{n}_{ECC}}{d\epsilon_s d\Omega_{obs}} = \frac{r_e^2\sigma_T K}{16\pi}\frac{\Gamma(3)\zeta(3)}{\Gamma^3}\int_1^\infty \frac{d\gamma}{\gamma^2}\int_0^{2\pi} d\phi_{ph}\int_{-1}^1 d\eta_{ph}\left[\frac{\Theta_D}{1+\beta_\Gamma\eta_{ph}}\right]^3$$
$$\times \left(\frac{\epsilon_s}{<\epsilon>}\right)^2 \sum_i \frac{1}{1-\beta\mu_i} n_{e,i}(\gamma)\frac{1}{|f'(n_{e,i})|}\left(\frac{<\epsilon>(1-\beta\mu_i)}{\epsilon_s(1-\beta\mu_{obs})} + \frac{\epsilon_s(1-\beta\mu_{obs})}{<\epsilon>(1-\beta\mu_i)} - \sin\chi'^2\right)$$
$$\times \int_{r_{in}}^{r_{out}} dr \frac{n_{blr}(\vec{r})d}{r^2|r-\eta_D^* z|} \ , \tag{110}$$

where μ_i, $\sin\chi'$, and κ are given by equations 77, 78, and 79, respectively.

As in §3.3, we have derived an expression that assumes a spherical geometry for the BLR. We can again accomodate a disk wind geometry with opening angle θ_{wind} by rearranging the order of integration. Then we have

$$\frac{d^2\dot{n}_{ECC}}{d\epsilon_s d\Omega_{obs}} = \frac{r_e^2\sigma_T K}{16\pi}\frac{\Gamma(3)\zeta(3)}{\Gamma^3}\int_1^\infty \frac{d\gamma}{\gamma^2}\int_0^{2\pi} d\phi_{ph}\int_{r_{in}}^{r_{out}} dr \frac{n_{blr}(\vec{r})d}{r^2|r-\eta_D^* z|}$$
$$\times \int_{\eta_{ph,min}}^{\eta_{ph,max}} d\eta_{ph}\left[\frac{\Theta_D}{1+\beta_\Gamma\eta_{ph}}\right]^3 \left(\frac{\epsilon_s}{<\epsilon>}\right)^2 \sum_i \frac{1}{1-\beta\mu_i} n_{e,i}(\gamma)\frac{1}{|f'(\eta_{e,i})|}$$
$$\times \left(\frac{<\epsilon>(1-\beta\mu_i)}{\epsilon_s(1-\beta\mu_{obs})} + \frac{\epsilon_s(1-\beta\mu_{obs})}{<\epsilon>(1-\beta\mu_i)} - \sin\chi'^2\right) \ , \tag{111}$$

where $\eta_{ph,min}$ and $\eta_{ph,max}$ are defined as in equation 108.

4. Summary

We have derived expressions for the single electron energy loss rates and emitted spectra due to inverse Compton scattering of two external sources of seed photons, accretion disk photons incident directly on the jet (ECD) and disk photons that first scatter off the BLR (ECC). Most of the derived equations use very few approximations, although we have also included simplified expressions that are valid in the Thomson regime. These equations form the basis for a code we are developing to model the leptonic emission processes relevant to the inner jets of blazars.

We are grateful to M. Böttcher for useful discussions and feedback on the derivations presented here.

A. Relativistic transformation equations

Here we collect two essential equations, used repeatedly in this paper, that describe the relativistic transformation of energies and angles. When transforming between relativistically-moving systems, we must account for two effects on photons (*cf.* equation 21 on page 59 of Heitler (1984)). First, the Doppler effect gives the relationship between the energy of the photon in a stationary system and its energy in a moving system; for a system moving with speed $\vec{\beta} = \frac{\vec{v}}{c}$:

$$\nu' = \nu \, \frac{1 - \beta \cos\theta}{\sqrt{1 - \beta^2}} \ , \tag{A1}$$

where ν is the photon frequency, θ is the angle between the photon direction and $\vec{\beta}$, and the primed and unprimed values indicate the moving and stationary systems, respectively. The second effect is relativistic aberration; the relationship between the direction of the photon

in the moving frame and its direction in the stationary frame is

$$\cos\theta' = \frac{\cos\theta - \beta}{1 - \beta\cos\theta} \ . \tag{A2}$$

REFERENCES

G.R. Blumenthal and R.J. Gould, 1970, Phys. Rev., 42, 2, 237-270

M. Böttcher and C.D. Dermer, 2005, AA,302, 37-44

M. Böttcher, H. Mause, and R. Schlickeiser, 1997, AA, 324, 395-409

M. Böttcher and S.D. Bloom, 2000, ApJ, 119, 469-477

R.C. Hartman *et al.*, 2001, ApJ, 553, 683-694

R.C. Hartman *et al.*, 1999, ApJS, 123, 79-202

W. Heitler, 1984, *The Quantum Theory of Radiation*, 3rd edition

G. Rybicki and A. Lightman, 1979, *Radiative Processes in Astrophysics*

N.I. Shakura and R.A. Sunyaev, 1963, AA, 24, 337-355

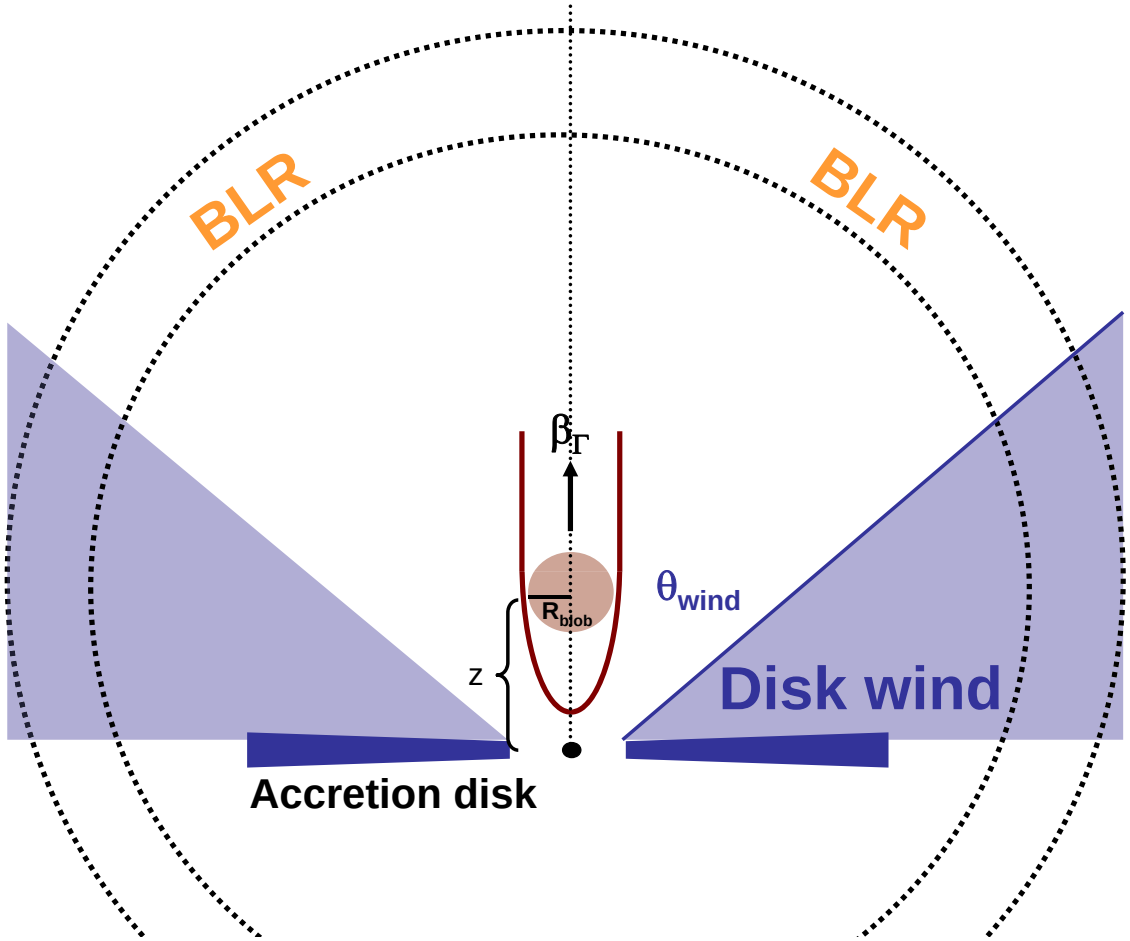

Fig. 1.— Cartoon of the large-scale view of the AGN, in which a blob of jet material of radius R_{blob} is ejected up away from the central black hole with bulk Lorentz factor Γ. Both the spherically-distributed cloud geometry and the disk wind geometry for the broad line region are depicted.

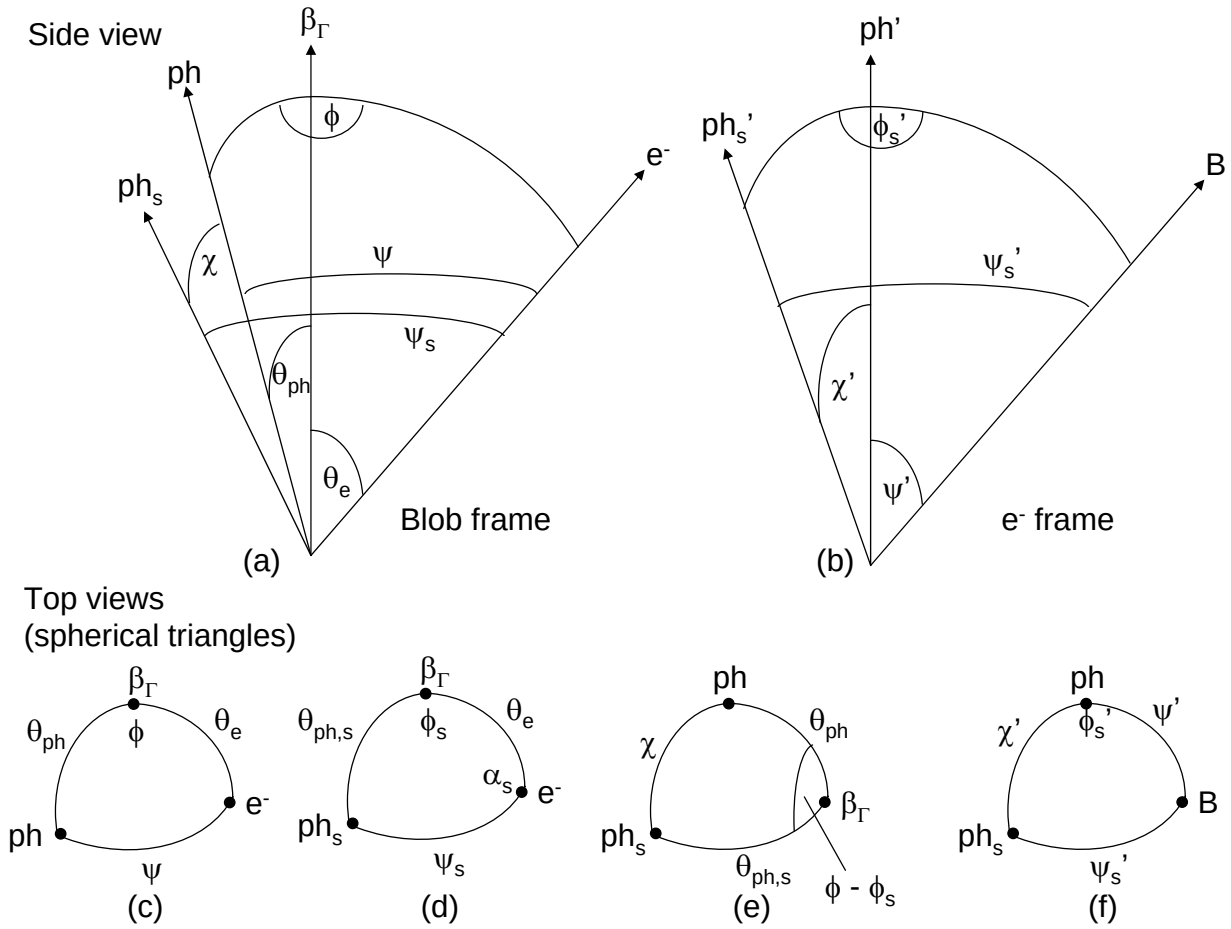

Fig. 2.— *top*: Side views of the geometry of the inverse-Compton scattering site, with the angles defined in two frames: the frame of rest of the blob (a) and the frame of rest of the electron in the blob (b). *bottom (c-f)*: The same angle definitions, with the spherical triangles viewed from above.

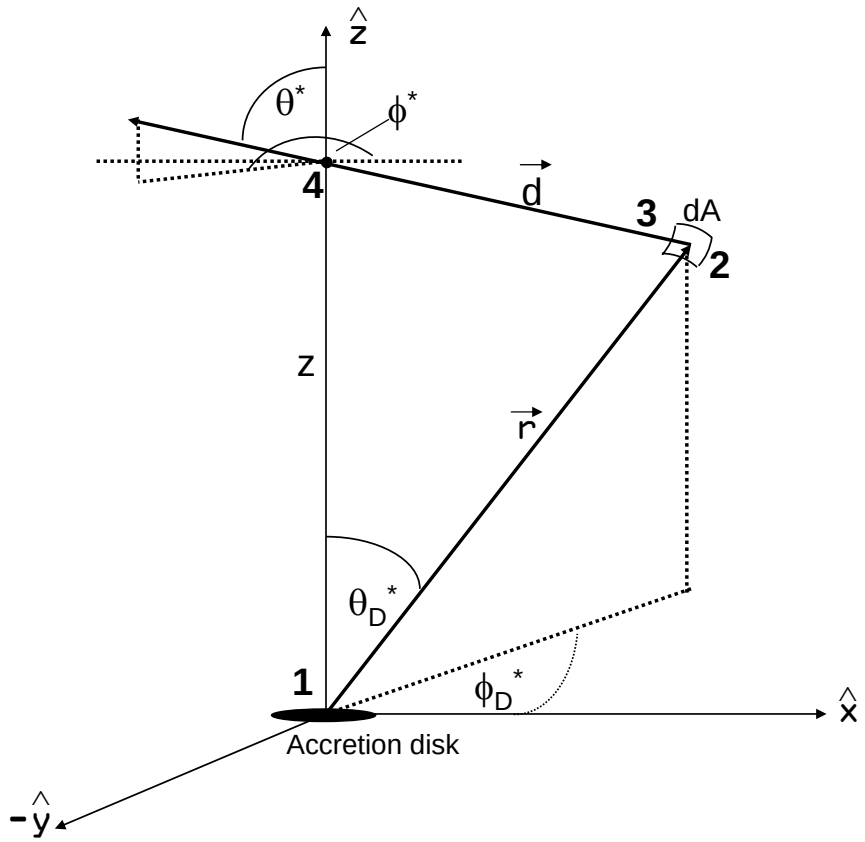

Fig. 3.— The broad line region (BLR) geometry. $\vec{r}$ is the distance to the BLR scattering site and z is the height of the blob above the disk. $\eta_D^* = \cos\theta_D^*$. Steps 1-4 are described in section 3.1.